

Review

Composites of Vegetable Oil-Based Polymers and Carbon Nanomaterials

Ana M. Díez-Pascual ^{1,*}  and Abbas Rahdar ² 

¹ Universidad de Alcalá, Facultad de Ciencias, Departamento de Química Analítica, Química Física e Ingeniería Química, Ctra. Madrid-Barcelona, Km. 33.6, 28805 Alcalá de Henares, Madrid, Spain

² Department of Physics, Faculty of Science, University of Zabol, Zabol 53898615, Iran; a.rahdar@uoz.ac.ir

* Correspondence: am.diez@uah.es; Tel.: +34-918-856-430

Abstract: Owing to current environmental concerns and crude oil price fluctuations, the design of feasible substitutes to petroleum-based polymeric materials is a major challenge. A lot of effort has been focused on transforming natural vegetable oils (VOs), which are inexpensive, abundant, and sustainable, into polymeric materials. Different nanofillers have been combined with these bio-based polymer matrices to improve their thermal, mechanical, and antibacterial properties. The development of multifunctional nanocomposites materials facilitates their application in novel areas such as sensors, medical devices, coatings, paints, adhesives, food packaging, and other industrial appliances. In this work, a brief description of current literature on polymeric nanocomposites from vegetable oils reinforced with carbon nanomaterials is provided, in terms of preparation, and properties. Different strategies to improve the nanomaterial state of dispersion within the biopolymer matrix are discussed, and a correlation between structure and properties is given. In particular, the mechanical, thermal, and electrical properties of these natural polymers can be considerably enhanced through the addition of small quantities of single-walled carbon nanotubes (SWCNTs), multi-walled carbon nanotubes (MWCNTs), graphene (G), or its derivatives such as graphene oxide (GO) or fullerenes (C₆₀). Finally, some current and potential future applications of these materials in diverse fields are briefly discussed.

Keywords: polymer nanocomposites; vegetable oils; carbon nanomaterials; fatty acids



Citation: Díez-Pascual, A.M.; Rahdar, A. Composites of Vegetable Oil-Based Polymers and Carbon Nanomaterials. *Macromol* **2021**, *1*, 276–292. <https://doi.org/10.3390/macromol1040019>

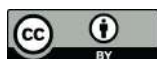
Academic Editor: Dimitrios Bikiaris

Received: 1 November 2021

Accepted: 23 November 2021

Published: 1 December 2021

Publisher's Note: MDPI stays neutral with regard to jurisdictional claims in published maps and institutional affiliations.



Copyright: © 2021 by the authors. Licensee MDPI, Basel, Switzerland. This article is an open access article distributed under the terms and conditions of the Creative Commons Attribution (CC BY) license (<https://creativecommons.org/licenses/by/4.0/>).

1. Introduction

Thermosetting polymers are insoluble polymeric materials that form a 3D network upon curing so that their properties can be easily tuned by adjusting the crosslink density. Most commercial thermosets, such as phenolic resins and epoxies, are produced from petroleum sources, but this is currently restricted due to depletion of fossil oils, global warming, and environmental concerns, as well as the growing price of crude oils [1]. Therefore, strong efforts have been devoted towards the development of sustainable, safe, and environmentally friendly plastics from renewable resources. However, the current practical use of renewable polymers is still very low mainly due to their poorer performance compared with synthetic polymers based on petroleum feedstock [2]. The main challenge is to design novel materials with properties comparable or even superior to those of petroleum-based ones. A variety of starting materials including polysaccharides, vegetable oils (VOs), lignin, pine resin derivatives, and proteins, have been used to synthesize renewable polymeric materials [3,4]. Among these, VOs, which are esters formed between glycerol and three fatty acids, are the most widely used due to their inherent biodegradability, easy availability, low toxicity, and relatively low price [5]. Taking into account the functional groups in VOs, such as esters and carbon-carbon double bonds in the fatty acid chains, numerous thermosets have been synthesized from vegetable oils via crosslinking of the triglycerides by free-radical or cationic polymerizations or condensation reactions, to produce various types of polymers, such as polyesters, polyamides, epoxies,

and polyurethanes (PUs). Furthermore, linseed and tung oil have been used for coating ingredients in oil paints and varnishes. These oils are heated thermally to prepare paint ingredients via a Diels–Alder reaction. These polymers are mainly used in the food industry but also as adhesives, foams, coatings, insulators, binders, in biomedicine (tissue engineering, medicinal sutures, wound healing, etc.), and as matrixes for the preparation of composites [6].

Nonetheless, polymers derived from VOs typically show poor mechanical and barrier properties, including brittleness, high gas and vapor permeability, and low heat distortion temperature, which limits their real applications [2]. To address these issues, different approaches have been described, such as mixing with other polymers [7], incorporating nanofillers [8–11], or the plasma treatment of the VOs or the carbon nanomaterials [8,9], which leads to bio-nanocomposites with improved performance. Specifically, their antimicrobial activity can be improved through incorporation of metal, metal-oxide nanoparticles, or carbon nanomaterials [12–14]. Moreover, enzymatic catalysis has been recently used for the modification and polymerization of VOs and their derivatives [15].

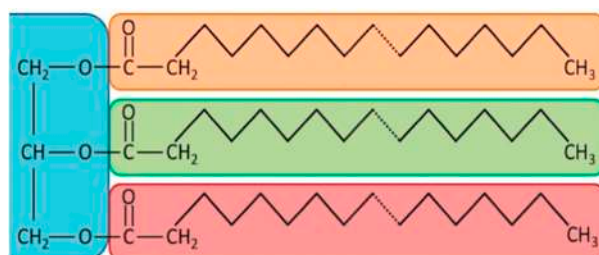
Over the last years, a few reviews dealing with polymeric materials derived from vegetable oils have been published [2–4]. However, very scarce studies have dealt with polymeric nanocomposites derived from thermosetting vegetable oils [6,9]. In this article, the synthesis, properties, and applications of polymeric nanocomposites based on epoxidized vegetable oils reinforced with carbon-based nanomaterials such as carbon nanotubes, graphene, and its derivative graphene oxide, and fullerenes are reviewed. The idea is to provide a brief overview of the current state-of-art in this arena, in order to encourage additional research on the design and manufacturing of this type of green nanocomposites.

2. Polymers Obtained from Vegetable Oils

VOs can be used as the source materials for polymers since they present numerous advantages compared to conventional plastics derived from fossil fuels such as inexpensiveness, biodegradability, biocompatibility (non-toxicity), easy availability, and abundance in nature [3]. Furthermore, they are sustainable and reduce environmental pollution such as greenhouse gas emissions (i.e., CO₂). They have a low density and high weight/volume ratio. Films of VOs can be produced by conventional techniques used for traditional polymers such as solution casting technique using water as a solvent, and they can be shaped into different forms. They can be stronger and lighter than conventional plastics such as polypropylene (PP), polystyrene (PS), or polyethylene (PE). Their processability and properties (i.e., thermal and mechanical) can match or even exceed the performance of conventional plastics, which combined with their environmental friendliness makes them highly attractive for a wide range of applications.

VOs contain triglycerides (Scheme 1) resulting from the esterification of glycerin and various fatty acids containing from 8 to 24 carbon atoms and between 0 and 7 carbon-carbon double bonds, depending on the plant type, weather conditions of growing, season, and purification methods [4]. The structures of the most common fatty acids found in VOs are summarized in Table 1. According to the presence or the absence of double bonds, they can be divided into saturated (SFAs—without double bonds), monounsaturated (MUFAs—with one double bond), and polyunsaturated fatty acids (PUFAs—with two or up to six double bonds). They are designated as x:y, where x is the number of carbons in the chain and y is the number of double bonds. Further, they are named as *cis* or *trans* based on the configuration of the double bonds and as n-3 or n-6 PUFAs based on the position of the first double bond from the fatty acid methyl-end. The human body cannot synthesize PUFAs with the first double bond on C3 and C6 from the methyl-end owed to the absence of suitable enzymes. Thus, these fatty acids are essential and have to be acquired from a diet. The most common are palmitic acid, linoleic acid, and stearic acid. Most of them exhibit a straight chain with an even number of carbons and double bonds in a *cis* configuration. Overall, the reactivity of carbon-carbon double bonds in VOs can be

increased upon conjugation. Thus, the term “conjugated oil” refers to oils in which most of the carbon-carbon double bonds are conjugated.



Scheme 1. Chemical structure of a triglyceride.

Table 1. Most common fatty acids in vegetable oils: formula, nomenclature, and structure.

Fatty Acid	Formula/ Nomenclature	Structure
Palmitic	$C_{16}H_{32}O_2$ /C16:0	
Palmitoleic	$C_{16}H_{30}O_2$ /C16:1 n-7	
Stearic	$C_{18}H_{36}O_2$ /C18:0	
Oleic	$C_{18}H_{34}O_2$ /C18:1 n-9	
Linoleic	$C_{18}H_{32}O_2$ /C18:2 n-6	
Linolenic	$C_{18}H_{30}O_2$ /C18:3 n-3	
α -Eleostearic	$C_{18}H_{30}O_2$ /C18:3 n-5	

Table 2 gathers the amounts of the different fatty acids in the most common VOs. The physicochemical properties of VOs are greatly dependent on the level of unsaturation, which can be obtained by calculating the iodine value (IV), which indicates the amount of iodine (mg) that reacts with the C=C double bonds in 100 g of the VOs; the greater the iodine value, the more unsaturation and the higher the susceptibility to oxidation. Peanut (PNT) oil (IV 80–106) is more saturated than corn (COR, IV 102–130), cotton (CTO, IV 90–119), or linseed (LO, IV 168–204) oils; nonetheless, it is significantly less saturated than palm (PO, IV 44–58). The IV values of the most widespread VOs are also collected in Table 2.

Soybean (SB), rapeseed (RPS), and PO are the VOs with the largest global production. Most of the global SB oil supply is produced in America, while RPS production predominates in Europe and PAL in Asia. Olive (OL), RPS, LO, castor (CO), SB, CTO, and sunflower (SFL) are the most commonly utilized for the synthesis of biopolymers [6,16] and can be used in fields ranging from lubricants and coatings to biodiesel and cosmetic products. Despite some VOs containing reactive functional groups such as OH (CST), which can be used directly for polymerization, applications are limited owing to the relatively low functionalities. Therefore, many VOs have to be modified before their use as monomers for polymer synthesis, which can be attained via chemical modification of the reactive sites of triglycerides (e.g., ester groups and carbon-carbon double bonds), following pathways similar to those applied for synthetic polymers [17]. Besides, polymers derived from VOs have poor mechanical and barrier properties, which limit their commercial uses. To solve these concerns, rigid nanofillers including metal nanoparticles, metal oxides, and carbon-based nanomaterials can be incorporated into the polymeric chains [8–11]. The following sections will present the most representative examples of polymer nanocomposites based on VOs and carbon nanomaterials. Polyurethanes (PUs), one of the most important classes of polymers, will be briefly discussed.

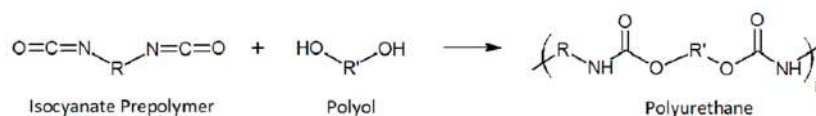
Table 2. Properties and fatty acid composition of the most common vegetable oils (VOs).

VO	DBPT ^a	IV ^b (mg/100 g)	C16:0 (%)	C18:0 (%)	C18:1 n-9 (%)	C18:2 n-6 (%)	C18:3 n-3 (%)
CN	7.9	110–126	6.0	-	4.0	9.0	-
CO	4.8	83–88	1.3	1.2	4.0	5.2	0.3
PNT	3.4	80–106	11.4	2.4	48.3	31.9	-
PO	1.7	44–58	42.8	4.2	40.5	10.1	-
LO	6.6	168–204	5.5	3.5	19.1	15.3	56
OL	2.8	75–94	13.7	2.5	71.1	10.0	0.6
SO	4.6	117–143	11.0	4.0	23.4	53.3	7.8
RPS	3.8	94–120	4.0	2.0	56.0	26.0	10
SES	3.9	103–116	9.0	6.0	41.0	43.0	1.0
CTO	3.9	90–119	21.6	2.6	18.6	54.4	0.7
COR	4.5	102–130	10.9	2.0	25.4	59.6	1.2
SFL	4.7	110–143	5.2	2.7	37.2	53.8	1.0

^a Average number of double bonds per triglyceride. ^b Iodine value: the amount of iodine (mg) that reacts with the double bonds in 100 g of vegetable oil. OL—olive; RPS—rapeseed; LO—linseed; CO—castor; SO—soybean; PNT—peanut; PO—palm; SES—sesame; CTO—cotton; SFL—sunflower; COR—corn; CN—canola.

2.1. Polyurethanes

PU are very versatile and show a wide range of properties and applications as coatings, adhesives, elastomers, foams, and so forth. They can be synthesized by polyaddition of polyisocyanates (typically a diisocyanate) and polyols (i.e., polyester or polyether polyol) (Scheme 2) which leads to urethane linkages in the backbone (–NH–C(=O)–O–) [18].

**Scheme 2.** Reaction between diisocyanate and polyol to form a polyurethane.

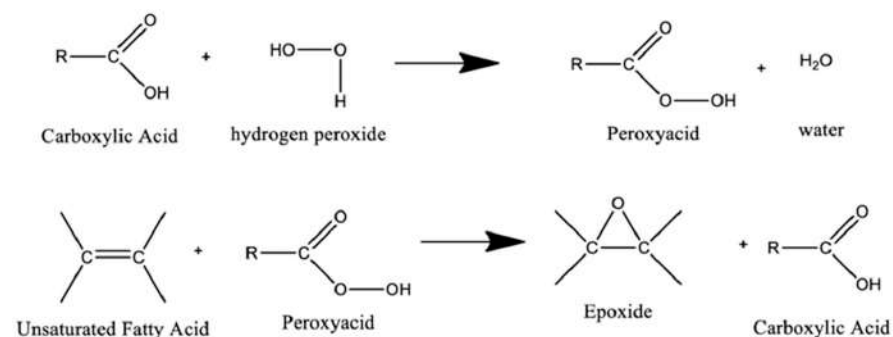
VOs with aliphatic chains are used to yield polyols which can be combined with isocyanates to form PUs with good elasticity, mechanical strength, toughness, and resistance to degradation [19]. For instance, Gurunathan et al. [20] synthesized a PU by reacting isophorone diisocyanate and CST. The glass transition temperature, Young's modulus, and tensile strength of the resulting PU increased with increasing isocyanate content owed to stronger hydrogen bonding. Meanwhile, the hydrophobicity of PU increased with increasing CST oil content.

Recently, epoxidation/oxirane ring-opening methods have been extensively investigated for the preparation of commercial VO-based polyols for PU production [21]. These methods involve two steps: epoxidation of unsaturated bonds that are present in the fatty acid chains followed by a ring-opening reaction of the oxirane groups using nucleophilic reagents, such as amines, carboxylic acids/halogenated acids, or alcohols. Water, alcohols, and in some cases, amines can be used as nucleophilic reagents for ring-opening of epoxides, a reaction that is often catalyzed with inorganic acids, such as phosphoric acid, sulphuric acid, fluoroboric acid, and Lewis acids [22].

2.2. Epoxidized Vegetable Oils

The epoxidation of vegetable oils is a renowned reaction since 1946 and nowadays, it is becoming very popular due to the high reactivity of the epoxy group. These functionalities can be introduced on unsaturation sites of VOs via chemical reactions such as the epoxidation of alkenes with in situ-generated peroxyacids (Scheme 3) [22]. However, it was reported that H₂O₂ and oil showed low reactivity in the absence of catalysts. In addition to H₂O₂, organic hydroperoxides are suitable oxidants for epoxidation reactions catalyzed by transition metals such as Mo and Ti. These metals with a strong Lewis acid

character are readily available catalysts. Peroxyacids such as performic acid, peracetic acid, and perpropionic acid are frequently chosen as oxygen carriers in the presence of H_2O_2 and inorganic acid catalysts (H_2SO_4 , H_3PO_4 , and HNO_3).



Scheme 3. Conventional epoxidation of vegetable oils. Reprinted with permission from ref. [22]. Copyright 2017 A. S. Belousov.

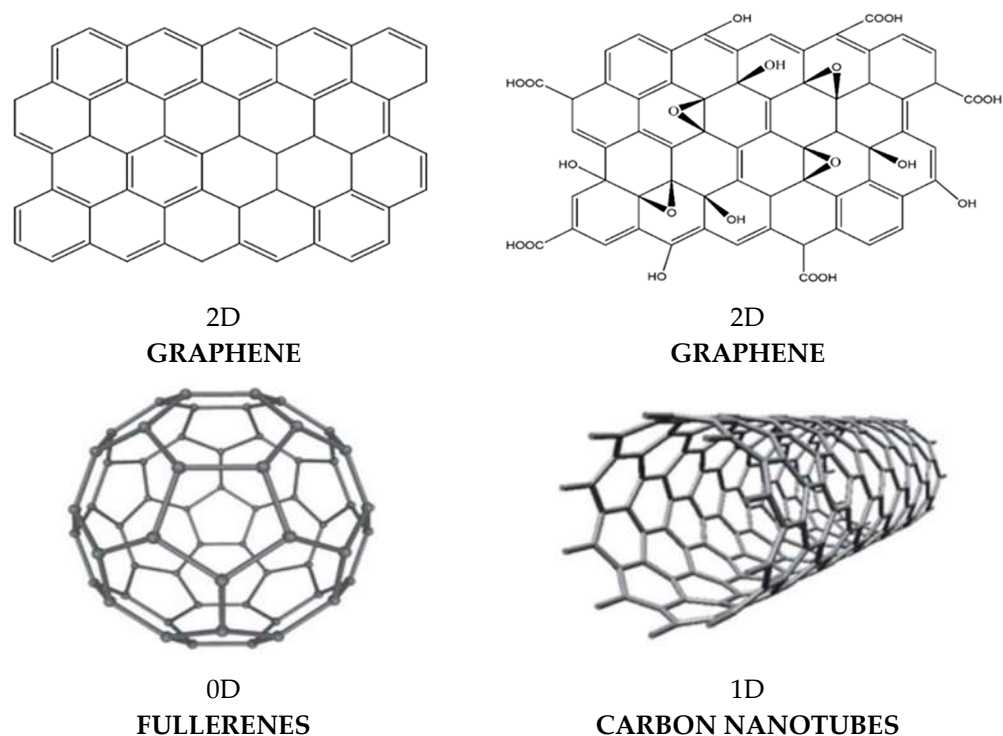
The main advantages of the VOs conventional epoxidation are the high yield of the process, the economic price of the reagents, and its good stability under epoxidation parameters [23]. On the other hand, it presents different shortcomings. Firstly, low selectivity results from the side reactions, such as ring opening of the epoxides that causes the formation of by-products such as diols, hydroxy esters, and other dimers. Secondly, neutralization of the strong inorganic acid and aqueous carboxylic acids yields massive amounts of salt. Moreover, the reaction is highly exothermic, which can cause thermal escape [24]. Enzyme-catalyzed epoxidation provides a new path for making epoxidized VOs and has numerous advantages compared to chemical processes, including mild reaction conditions, i.e., room temperature, high stereoselectivity, Thirdly, high yield, and elimination of side reactions. Thus, using a commercial enzyme and H_2O_2 as oxidizing agents, high selectivities and conversion yields (above 90%) have been attained for epoxidation of RPS, LO, SB, and SFL oils in 10 h [25].

3. Polymer Composites from Vegetable Oils

In order to enhance the properties of VOs, different types of micro and nanoscale fillers including glass fibers [26], nanoclays [27], metal oxide nanoparticles [10,13,28], and carbon nanomaterials [29–34] have been incorporated into these matrices. Amongst them, carbon nanomaterials such as carbon nanotubes (CNTs), fullerenes, graphene (G), and its derivatives such as graphene oxide (GO) have attracted a lot of attention due to their unique structural dimensions and excellent mechanical, electrical, thermal, optical, and chemical properties.

CNTs are rolled-up sheets of single-layer carbon atoms with sp^2 hybridization (Scheme 4) [14]. They can be divided into two main types: single-walled carbon nanotubes (SWCNTs), seamless cylinders with only one carbon layer, or multi-walled carbon nanotubes (MWCNTs), with multiple concentric carbon layers weakly bound together by van der Waals interactions. They have low density (1.3 to 1.4 g/cm^3) and outstanding stiffness and strength (i.e., 63 GPa), as well as very high electrical and thermal conductivity (more than 1000 times greater than those of metals such as Cu). However, they have a great tendency to aggregate and form bundles, which results in a significant worsening of properties, including mechanical and electrical. Henceforward, functionalization with polymers [35,36] or other molecules is usually carried out.

Fullerenes are carbon nanospheres with a hollow structure and possess sp^2 and sp^3 hybridized carbon atoms. The most commonly known is C_{60} , named Buckminster fullerene [37]. Its structure is a truncated icosahedron, which resembles a football ball made of twenty hexagons and twelve pentagons. Due to delocalized π electrons, fullerenes have nonlinear optical responses and high electron affinity.



Scheme 4. Structure of carbon nanomaterials: 2D graphene and its derivative graphene oxide (GO), 0D fullerenes, and 1D carbon nanotubes (CNTs). Reprinted from ref. [14].

G is a 2D atomically flat monolayer of carbon atoms with sp^2 hybridization and exceptional properties, including mechanical, thermal, and electrical. It is the stiffest material on earth, hardest than steel, and has higher electrical conductivity than metals including Cu. It also has molecular barrier ability, low density, and very little toxicity [38]. Nonetheless, the use of pristine G has been limited due to its intense aggregation tendency, as well as its hydrophobicity, which leads to insolubility in aqueous media. Consequently, derivatives such as GO have been manufactured. GO is attained via oxidation of G, and includes acid groups on the edges and epoxide, hydroxyl, and ketone groups on the basal planes (Scheme 3). It is soluble in aqueous media and is amphiphilic. It can also be reduced to yield reduced graphene oxide (rGO) [39].

3.1. Vegetable Oil-Composites Incorporating Carbon Nanotubes

CNTs have been used as reinforcements in numerous synthetic polymer matrices for high-performance nanocomposites owed to their excellent mechanical properties and electrical and thermal conductivity [40–43]. Synthetic polymer matrices can be replaced by VO-based polymer for the development of biocompatible and biodegradable nanocomposites. For instance, it was found that the addition of 0.28% MWCNTs to acrylated epoxidized soybean oil (AESO)-based resin led to a 30% increase in modulus, while higher MWCNT contents led to significant aggregation, hence a reduction in properties. Furthermore, an optimal polymer-MWCNT interfacial adhesion was observed via TEM images [29]. Nanocomposites of AESO/styrene in a 65/35 wt.% ratio incorporating 3 wt.% SWCNT loading were also prepared [44] by sonication method followed by polymerization via free radicals using tert-butyl peroxy benzoate as initiator. It was found that the SWCNT significantly increase the mechanical properties: the flexural modulus and strength by about 45% and 10%, respectively, and the glass transition temperature by about 8%. However, hardly any change in thermal stability was observed. Recently, AESO has also been grafted on the surface of MWCNTs by reversible addition-fragmentation chain-transfer reaction (RAFT) [45]. MWCNTs-AESO as reinforcement have been used to develop epoxidized soybean oil/maleopimaric-based thermosetting composites with good dispersion via probe

ultrasonic treatment in ethyl acetate. Morphological observations via SEM and TEM corroborated that MWCNTs-AESO had improved dispersion within the epoxy matrix than the MWCNTs alone and stronger interfacial bonding, and this resulted in a synergistic effect on enhancing the mechanical performance of the matrix. Besides, significant increases in the glass transition temperature were observed. Other authors incorporated MWCNTs with different diameters into the ESO-PU matrix and found that the larger diameter ones were more easily dispersed than the smaller-diameter due to the weaker van der Waals interactions between the tubes resulting in better properties such as higher tensile strength, elastic modulus, ductility, and thermal conductivity [32]. In addition, soy-based PU foams reinforced with 0.5 and 1.0 wt.% MWCNTs were developed [34]. At 0.5 wt.% MWCNT, the compressive, flexural, and tensile properties of MWCNTs-VO based foams were improved by 24%, 30%, and 30%, respectively, as compared with the neat resin, attributed to the fact that the MWCNTs acted as nucleation sites and promoted an efficient load transfer to the polymer network. However, this process was hindered at higher loadings due to MWCNT aggregation.

On the other hand, environmentally friendly nanocomposites were developed with epoxidized linseed oil (ELO) as green matrix and polyaniline (PANI) and MWCNTs as conductive fillers. Two different concentrations of MWCNTs (0.1 and 0.4 wt.%) were added to ELO/PANI composites [46]. The electrical conductivity showed a maximum of 4.5×10^{-5} S/cm at 0.4 wt.% loading, corroborating the synergist effect of both fillers on enhancing the conductivity. The homogeneous distribution of both CNT and PANI in the ELO matrix was confirmed by SEM analysis (Figure 1). The glass transition temperature, storage modulus, tensile strength, impact strength, and Young's modulus increased upon increasing CNT loading.

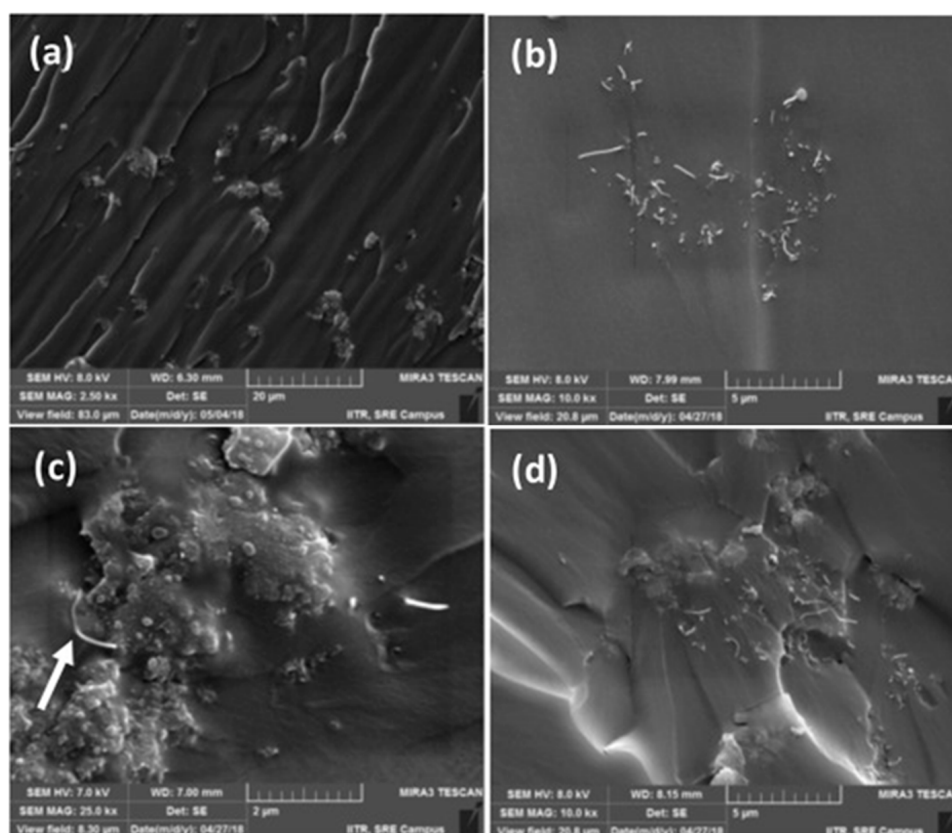


Figure 1. SEM micrographs of (a) ELO/PANI composite, (b) ELO/MWCNT (0.1 wt.%) composite, (c,d) ELO/PANI/MWCNT (0.1 wt.%) composite. Reprinted with permission from ref. [46]. Copyright 2019 Gaurav Manik.

ELO-based nanocomposites reinforced with fluorinated single-wall carbon nanotubes (FSWCNTs) were also developed [31]. The addition of 0.24 wt.% FSWCNTs into the matrix decreased the glass transition temperature by about 30 °C, while strong improvements in the storage modulus (up to 14%) and in the fracture toughness (up to 43%) were attained compared to the neat ELO resin. It is interesting that excellent improvement in stiffness was achieved without sacrificing the toughness.

Ali et al. synthesized CO-based PU nanocomposites reinforced with MWCNTs, in the range of 0–1 wt.%. The MWCNTs were purified via acid treatment, which resulted in the formation of –OH, –NH, and –C=O groups on the CNT surface. About 130% increase in modulus and 5% increase in tensile strength was found for an MWCNT loading of 0.3 wt.% [47] since the tubes were very homogeneously distributed within the VO-based matrix. At higher concentrations, the nanotubes aggregated, as revealed by SEM analysis. The nanocomposite with 0.3 wt.% also showed the best thermal stability, showing about 50 °C increase in the thermal decomposition temperature, ascribed to the combined effect of excellent thermal stability of MWCNTs and their strong interfacial interactions with the VO matrix. On the other hand, the nanocomposite with 5 wt.% MWCNT displayed the best barrier properties, about 70% reduction in nitrogen permeability compared to the neat polymer, likely due to the exfoliation, compatibilization, orientation, and reaggregation of purified MWCNTs into the polymer matrix. The FTIR spectrum showed a shift in the peak related to CO with increasing MWCNT loading, related to carbonyl hydrogen bonding in the nanocomposites (Figure 2). The carboxylic acid groups of the purified MWCNTs may have reacted with OH groups of the polymer to form ester groups, and this covalent bonding accounts for the strong property improvements observed.

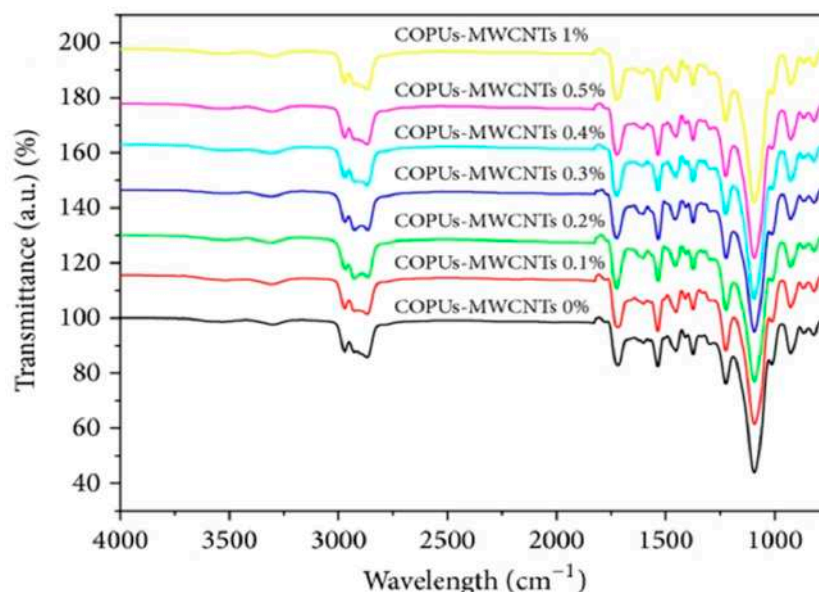


Figure 2. FT-IR spectra of pure CO-based PU and nanocomposites with different MWCNT loading. Reprinted from ref. [47].

Soy-castor oil-based PU nanocomposites reinforced with silane-modified multiwalled carbon nanotubes (s-MWCNT) were successfully prepared [30]. The MWCNTs were modified by amine moieties by silanization and incorporated in the matrix via covalent bonding. The effect of s-MWCNT loading on the morphology, thermomechanical, and tensile properties of the PU nanocomposites was investigated. The storage modulus, glass transition temperature, Young's modulus, and tensile strength of the nanocomposites increased with increasing s-MWCNT content up to 0.8 wt.%. However, at higher loadings, a worsening in properties was found ascribed to a competition between the amine and hydroxyl groups for the isocyanate groups of the PU-based VO. High s-MWCNT contents

also induced nanotube aggregation, which is detrimental to property improvement. Hyper-branched CO-based PU nanocomposites with MWCNTs as reinforcement and poly (ϵ -caprolactone)diol as the soft segment were also prepared by in situ polymerization [33]. At 2 wt.% loading, the mechanical and shape memory properties were significantly improved.

3.2. Vegetable Oil-Composites Incorporating Graphene and Its Derivatives

Soybean oil-based PU nanocomposites with 1 wt.% of three different types of functionalized graphene: dispersible graphene (G), reduced graphene oxide with amine groups (rGO-NH₂), and reduced graphene oxide-tetraethylene pentamine (rGO-TEPA) were developed [48]. SEM images (Figure 3) revealed the quite homogeneous dispersion of G nanosheets in the PU-VO matrix. The nanocomposite with 1 wt.% dispersible graphene exhibited a 75% increment in storage modulus at 25 °C, a 34% increase in tensile strength, and a 30% increase in Young's modulus. Furthermore, improvement in thermal stability was also observed.

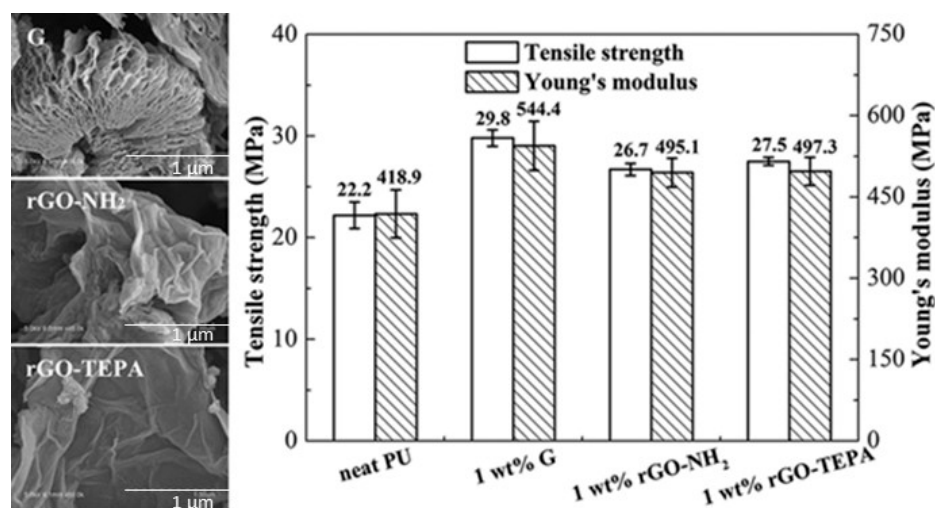


Figure 3. SEM images (left) of SO-PU nanocomposites reinforced with G, rGO-NH₂ and RGO-TEPA. Tensile strength and Young's modulus of the nanocomposites with 1 wt.% loading of G, rGO-NH₂ and RGO-TEPA. Reprinted with permission from ref. [48]. Copyright 2015 Hongfeng Xie.

AESO-CO-based PU composites with GO as nanofiller have been prepared using a modified pressurized oxidation method and were investigated using Raman spectra, AFM, and XPS, respectively [49]. The addition of GO (0.4 wt.%) in the PU matrix led to a 130% increase in elongation at break and an 80% increase in toughness. However, the results from the thermal analysis indicated that the GO acts as a soft segment in the polyurethane which leads to a considerable decrease in the glass transition temperature and crosslink density. SEM images showed a considerable GO aggregation at concentrations above 0.4 wt.%.

AESO-based composites with functionalized graphene or graphene oxide have been prepared using a UV curing technique [50]. Graphene (GN) and graphene oxide (GO) were chemically functionalized with 3-methacryloxypropyltrimethoxysilane and 4,4'-diphenylmethanediisocyanate/hydroxyl ethyl acrylate, respectively, and used as filler in the AESO matrix. IR (Figure 4) and X-ray photoelectron spectroscopy (XPS) confirmed the functionalization of GN and GO and the formation of polymer networks in the composite. Thus, the stretching vibrations of -NH-groups at 3390 cm⁻¹ together with the carbonyl bands at 1705 cm⁻¹ corroborate the formation of the urethane bond. The disappearance of the peak related to the isocyanate group at 2264 cm⁻¹ also confirms the covalent bonding. Functionalization was effective in improving filler dispersion into the polymer matrix, which led to significant improvement in mechanical properties (-48% increase in tensile

strength with 0.02% FGN), while the AESO composites with raw GN or GO exhibited lower tensile strengths.

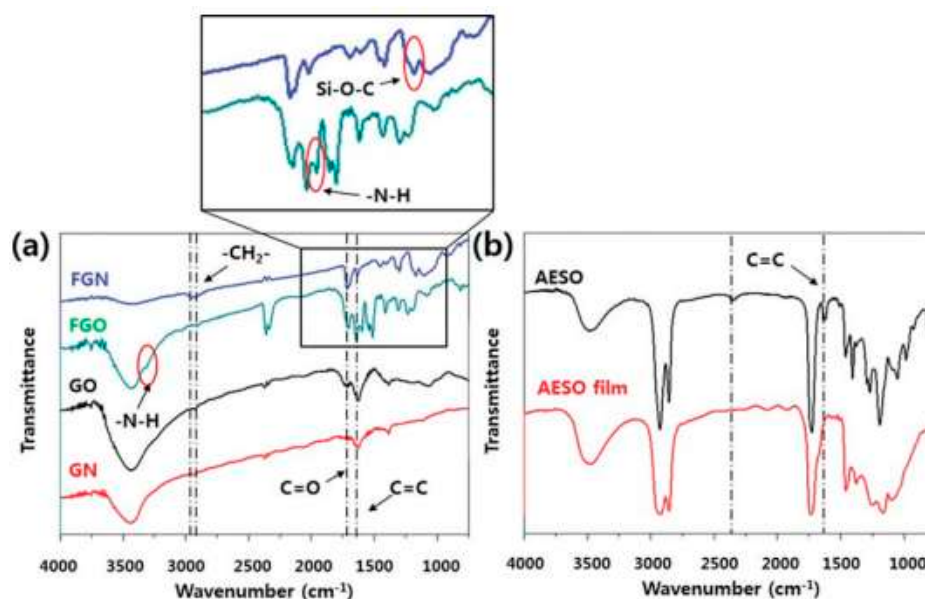


Figure 4. FTIR spectra of (a) graphene oxide (GO), graphene (GN), functionalized graphene oxide (FGO), functionalized graphene (FGN), (b) AESO, and AESO film. Reprinted with permission from ref. [50]. Copyright 2019 Beom Soo Kim.

CO-based hyperbranched PU nanocomposites with 0.5, 1.0 and 2.0 wt.% GO as reinforcement have also been prepared [51]. An unprecedented improvement in toughness (160%), as well as a strong increase in tensile strength (130%) and moderate improvement in elongation at break (15%), were attained. Furthermore, the nanocomposites showed excellent shape recovery (99.5%) and shape fixity (90%). The same authors prepared similar nanocomposites via an in situ polymerization technique [52], in which GO was reduced to rGO using a green sonochemical approach in the presence of *Colocasia esculenta* leaves extract. The nanocomposites (0.5–2.5 wt.% rGO) proved outstanding thermal stability and mechanical properties, including elastic modulus, tensile strength, and toughness, and showed excellent multi-stimuli responsive shape memory behavior.

Poly(lactide acid) (PLA) based nanocomposites with amphiphilic rGO functionalized with epoxidized methyl oleate were prepared via a solvent-free ring-opening reaction [53]. This environmentally friendly and scalable technique led to the oleo-rGO being well dispersed inside the matrix, which led to significant improvement in the mechanical properties of the nanocomposites. Thus, at room temperature, the storage modulus of oleo-rGO/PLA was about double that of neat PLA, while the glass transition temperature decreased slightly. Moreover, a 22% increase in Young's modulus and a 6.2% rise in strength were found. G nanoplatelets were also explored as new nanoreinforcements for PLA/epoxidized palm oil (EPO) blend [54]. The ternary nanocomposites were developed via melt blending. A strong increase in strength and elongation at break (up to 26.5% and 60.6% respectively, at 0.3 wt.% loading) were found compared to the PLA/EPO blend. However, the incorporation of G nanoplatelets had no effect on the flexural strength and modulus. Impact strength of PLA/5 wt.% EPO improved by 74% upon the addition of 0.5 wt.% graphene loading. This was rationalized by a disorientation mechanism, as depicted in Figure 5. At very low G loadings (Figure 5a), the reinforcement effect is limited since the density of filler is not high enough to form a percolated network. Although complete randomization of the nanoplatelets was attained, no total graphene contact will be achieved since their spheres of rotation will not intersect.

For 0.3 wt.% G, the state of dispersion improves as the concentration increases, hence the mechanical properties improve, and a percolated network is formed (Figure 5b). Upon increasing loading, the tensile strength drops given that reorientation cannot be achieved due to excluded volume interactions between nanoplatelets (Figure 5c). When the amount of nanoplatelets reaches a critical concentration (0.3 wt.%), the distance between two nanoplatelets is so small that they stack together owed to Van der Waals forces, and this is reflected in lower tensile strength. Bio-composites from epoxidized *Jatropha curcas* oil with expanded graphite as filler have also been developed as flame retardant materials [55]. The incorporation of graphite, in particular 5 wt.%, improved the thermal and mechanical properties, slowed the degradation in phosphate buffer solution (pH 7.4), and also increased the limiting oxygen index of the bio-composites. The increase in thermal stability was ascribed to the restricted mobility of the polymeric chains in the presence of graphite.

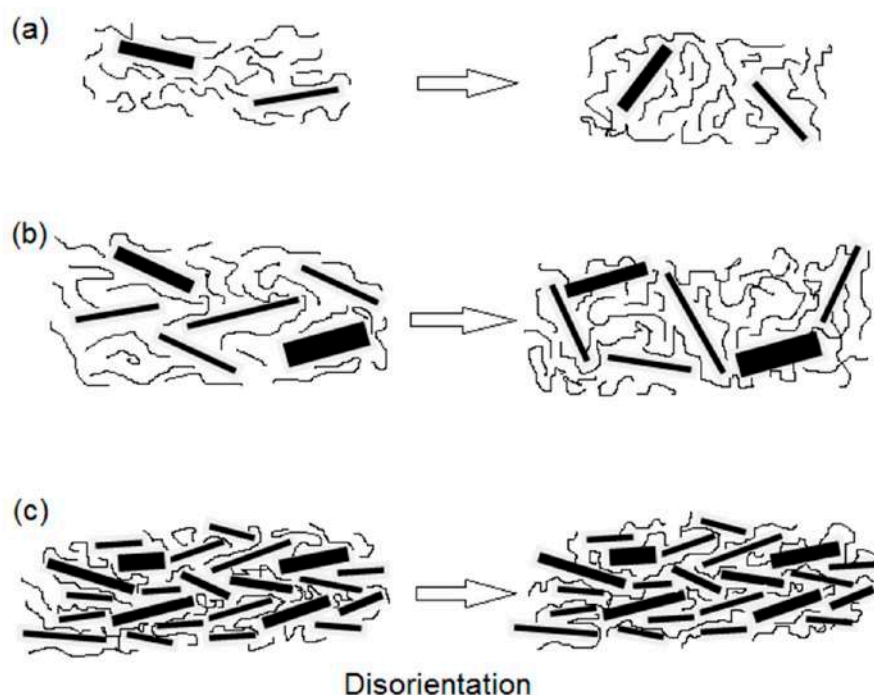


Figure 5. Illustration of disorientation mechanism of G nanoplatelets at (a) 0.1 wt.%; (b) 0.3 wt.% and (c) >0.5 wt.%. Reprinted from ref. [54].

3.3. Vegetable Oil Composites Incorporating Fullerenes

Despite the great potential of fullerenes, very few studies have accomplished the development of VO composites with this type of carbon nanomaterials. For instance, the addition of C_{60} in the oxidation stability of rapeseed oil has been studied. C_{60} (0–6 wt.%) was synthesized via the carbon arc method. Differential scanning calorimetry was applied to estimate the oxidation induction time of fullerene-oil composites. The addition of C_{60} significantly hampered the peroxide formation thus increasing of oxidation stability of rapeseed oil [56]. A recent article also investigated the improvement in the oxidation stability of esters derived from sunflower, soya, coconut, rape, and linen upon addition of 0.05 wt.% C_{60} , and it was proved that the aging process slowed down [57].

To obtain better insight into the property improvements attained in VO-based composites reinforced with carbon nanomaterials compared to those based on conventional commodity plastics such as PP, PS, or PE, the increments in mechanical properties compared to the neat matrix were calculated, and the values are collected in Table 3.

Table 3. Comparison of the mechanical properties of VO-based composites with carbon nanomaterials and those based on conventional plastics such as PP, PE, and PS.

Matrix	Nanofiller (wt.%)	E (% Δ)	σ (% Δ)	E_{flex} (% Δ)	σ_{Flex} (% Δ)	T_g ($^{\circ}C \Delta$)	T (% Δ)	Ref.
AESO	MWCNT (0.28)	30		-	-	-		[29]
AESO	SWCNT (3.0)	-		45	10	8		[44]
SO foam	MWCNT (0.28)	30		30	-	-	-	[34]
ELO	FSWCNT (0.24)			-	-	-30	43	[31]
CO	purified MWCNT (0.3)	130	5	-	-			[47]
SO	G (1.0)	30	34	-	-			[48]
SO	rGO-NH ₂ (1.0)	25	18					[48]
AESO-CO	GO (1.0)					-30	80	[49]
CO	GO (2.0)		130				160	[51]
PLA/EPO	G (0.3)		26.5				74	[54]
PP	MWCNT (0.75)	38	15					[58]
PS	MWCNT (0.26)	55	44					[59]
PE	g-MWCNT (0.26)	50	28				60	[60]
PP	G (1.0)	8	3				26	[61]
PS	GO (1.0)	40	25					[62]
PE	GO (0.3)	13	10.5				-5.5	[63]

E: Young's modulus; σ : tensile strength; E_{flex} : flexural modulus; σ_{Flex} : flexural strength; T_g : glass transition temperature; T: toughness; % Δ : percentage of increment; $^{\circ}C \Delta$: increment in degrees.

Regarding nanocomposites with MWCNTs, the largest modulus improvement was found upon the addition of 0.3 wt.% purified CNTs to CO [47], significantly larger than that found upon the addition of a similar amount of CNTs to PS or PE [59,60]. This strong improvement is attributed to very intense CNT-CO interactions via H-bonding between the amino and hydroxyl surface groups of the CNTs and the OH groups of the VO matrix. Furthermore, chemical bonding can be formed between the COOH on the MWCNT surface and the OH moieties of CO, and this accounts for the extraordinary reinforcement effect. Focusing on G and its derivatives, the highest increments (up to 130% and 160% in strength and toughness, respectively) was found upon the addition of 2 wt.% GO to CO [51], again due to the strong interactions between oxygenated functional groups of both nanocomposite components. Thus, it seems that modified carbon nanomaterials can interact more strongly with VOs than with hydrophobic polymers, resulting in significantly larger mechanical property improvements. The fact that VO-based composites can exceed the performance of conventional plastics derived from fossil fuels is highly interesting to solve the current environmental emergency connected to this type of plastics.

4. Applications of VOs with Carbon Nanomaterials

Most of the commercial applications of VO-based composites are related to the food industry, cosmetics and pharmaceuticals (cosmetics, creams, ointments, lotions), or paint and coating industry (coatings, adhesives, lubricants, foams, paints, etc.) [64]. Applications of rigid VO-based foams include insulations for tanks, pipes, water heaters, refrigerators, and freezers. Elastomeric VOs can also find many uses in the automotive industry. Moreover, due to the development of multifunctional nanocomposite materials, novel potential applications have emerged such as sensors, medical devices, tissue engineering, shape-memory materials, and so forth.

Among the various possible applications of oil-derived polymer composites, adhesives and coatings have received much attention. Thus, CO-based PU nanocomposites reinforced with MWCNTs show reduced hydrophobicity with increasing nanotube concentration and improved mechanical and impact properties, hence are suitable for use as protective coatings [51]. Moreover, they show very good gas barrier properties, hence can be used to develop films for active food packaging. On the other hand, the use of this type of composites as lubricants has also been explored. Thus, Kiu et al. [65] investigated the tribological effect of different contents of G (25, 50, and 100 ppm) in EPO. The results showed that 50 ppm is the optimum concentration that yielded the lowest wear scar

diameter and friction coefficient as compared to the control sample. CNTs have also been used as nano-additives in this matrix, providing good antiwear properties [66].

Low-density soy-based PU foams reinforced with 0.5 and 1.0 wt.% MWCNTs were developed [48] and showed improved compressive, flexural, and tensile properties. Semi-structural applications could benefit from the light weight and good mechanical properties of this type of foam, for example, for the manufacture of car interior panels or acoustic insulation panels for the construction industry, among others.

Some authors have considered the use of VOs-derived precursors to prepare shape-memory materials, that is, materials with the capability to modify their shape, by fixing a temporary shape and self-recovering their original dimensions on requirement as a response to an external stimulus [67]. In this regard, CO-based hyperbranched PU nanocomposites with 0.5, 1.0, and 2.0 wt.% GO as reinforcement have been prepared [51], showing extraordinary improvements in toughness and tensile strength. Besides, they showed outstanding shape recovery, which makes them excellent candidates for shape memory application. Similar nanocomposites were prepared by in situ polymerization technique [52], with exceptional multi-stimuli responsive shape memory behavior under direct sunlight, microwave, and heat energy. These nanocomposites have great potential to be used as triggered smart materials for diverse applications such as biomedicine. Thus, developing smart biomaterials with tailor-made properties is a key factor to successful tissue regeneration. Thus, it is envisioned that the developed CO/G nanocomposites might have a potential application in tissue engineering. Acid-modified MWCNTs and LO-based PU nanocomposites have also been reported and exhibited excellent shape recovery, enhanced biodegradability, and cytocompatibility, demonstrating their suitability as shape-memory biomaterials [68].

5. Conclusions and Future Perspectives

This review provides a brief description of current literature on polymeric nanocomposites from vegetable oils reinforced with carbon nanomaterials. Representative examples have been provided with the aim to shed light on their far range of applications from coatings, adhesives, lubricants, foams and paints to sensors, medical devices, tissue engineering, and shape-memory materials.

Vegetable oils constitute a rich and versatile feedstock for developing biopolymer-based composites. However, the main challenge for VO-based polymers is the performance gap compared to conventional petroleum-based polymers. Thus, currently, strong research struggles are being carried out to reduce these differences. Several strategies have been proposed to change these natural resources into multi-functional polymer composites with high modulus, strength, resistance, and flame retarding capability, suitable as an alternative to petroleum-based plastics. One strategy is the chemical modification of monomers, which can lead to improvements in the processing, thermal, and mechanical properties. Another approach is the incorporation of nanofillers including metal nanoparticles, metal oxides, and carbon-based nanomaterials to attain new properties and extend their application areas. Although some progress has been made, several challenges still exist. For instance, better strategies for dispersing the nanomaterials in the VOs matrices and for improving the design architecture to develop multifunctional composites are required. To date, many questions remain unanswered such as the effect of nanomaterial size, concentration, level of functionalization, and so forth on the final nanocomposite performance.

On the other hand, approaches to synthesize carbon nanomaterials at a large scale and at a low cost are pursued. Despite remarkable efforts that have been performed in this direction, up-to-date methods are restricted by their low productivities, and this is a shortcoming for practical applications. Yet, a trustworthy method to address the strong demand for G or CNT synthesis via a sustainable mean and with a high yield is absent. An additional drawback is that the actual specific surface area of carbon nanomaterials is considerably lower than the theoretical due to their strong agglomeration trend via Van der Waals interactions, and this restricts their properties. Thus, new strategies to effectively

disperse them in suitable solvents are pursued. Further, the toxicity of carbon nanomaterials is not well understood yet. Regardless of the substantial efforts in investigating the effect of these nanomaterials on human health, outcomes are frequently unreliable. They might cause toxicity in humans, and this point should be further clarified. In addition, the effects of carbon nanomaterials may differ depending on their intrinsic properties (shape, size, etc.).

On the other hand, a lot of research is now focusing on a new class of carbon-based nanomaterials: carbon quantum dots (CQDs), which are fluorescent and possess the attractive properties of high stability, good conductivity, biocompatibility, environmental friendliness, simple synthetic routes as well as comparable optical properties to quantum dots [69]. CQDs have been extensively investigated especially due to their strong and tunable fluorescence emission properties, which enable their applications in biomedicine, optoelectronics, catalysis, and sensing. It is expected that in the future, the combination of VOs with CQDs can lead to nanocomposites with very interesting properties in the aforementioned fields.

In summary, the perspectives for VO-based nanocomposites are very promising given the long-term need for substitutes to petroleum-based composites. However, currently is delayed by the lack of methods to offer easy, reproducible, and cost-effective nanomaterials at a large scale. The investigation in this arena is still in its initial stages. The mixture of carbon nanomaterials and VOs has opened novel properties and applications owed to synergistic effects. Nonetheless, more effort is required to guarantee that these nanocomposites are simple to develop and are non-toxic. Environmental and sustainability incentives promote the development of these bio-based nanocomposites that in some cases found their position in the market with difficulties because they had to compete with highly standardized fossil-based products. It can be foreseen that subsequently wide-ranging research in the field, commercial products containing VO-based nanocomposites that provide cost savings and minimize the performance differences compared to conventional polymers will be attained.

Author Contributions: A.M.D.-P. designed the work and wrote the article. A.R. contributed to literature review and editing. All authors have read and agreed to the published version of the manuscript.

Funding: Financial support from the Community of Madrid within the framework of the Multi-year Agreement with the University of Alcalá in the line of action “Stimulus to Excellence for Permanent University Professors”, Ref. EPU-INV/2020/012 is gratefully acknowledged.

Institutional Review Board Statement: Not applicable.

Informed Consent Statement: Not applicable.

Data Availability Statement: The data presented in this study are available on request from the corresponding author.

Conflicts of Interest: The authors declare no conflict of interest.

References

1. Gandini, A. The irruption of polymers from renewable resources on the scene of macromolecular science and technology. *Green Chem.* **2011**, *13*, 1061. [[CrossRef](#)]
2. Lligadas, G.; Ronda, J.C.; Galià, M.; Cádiz, V. Renewable polymeric materials from vegetable oils: A perspective. *Mater. Today* **2013**, *16*, 337–343. [[CrossRef](#)]
3. Babu, R.P.; O'Connor, K.; Seeram, R. Current progress on bio-based polymers and their future trends. *Prog. Biomater.* **2013**, *2*, 8. [[CrossRef](#)]
4. Raquez, J.-M.; Deléglise, M.; Lacrampe, M.-F.; Krawczak, P. Thermosetting (bio)materials derived from renewable resources: A critical review. *Prog. Polym. Sci.* **2010**, *35*, 487–509. [[CrossRef](#)]
5. Gunstone, F. *Fatty Acid & Lipid Chemistry*; Blackie Academic & Professional: New York, NY, USA, 1996; pp. 1–252. ISBN 978-1-4613-6852-6.
6. Belgacem, M.N.; Gandini, A. *Monomers, Polymers and Composites from Renewable Resources*; Elsevier: Amsterdam, The Netherlands, 2008; pp. 39–66. ISBN 9780080453163.

7. Wang, R.; Schuman, T.P. Vegetable oil-derived epoxy monomers and polymer blends: A comparative study with review. *Express Polym. Lett.* **2013**, *7*, 272–292. [[CrossRef](#)]
8. Multanen, V.; Chaniel, G.; Grynyov, R.; Loew, R.Y.; Siany, N.; Bormashenko, E. Hydrophilization of liquid surfaces by plasma treatment. *Colloids Surf. A* **2014**, *461*, 225–230. [[CrossRef](#)]
9. Chen, I.-H.; Wang, C.-C.; Chen, C.-Y. Preparation of Carbon Nanotube (CNT) Composites by Polymer Functionalized CNT under Plasma Treatment. *Plasma Process. Polym.* **2010**, *7*, 59–63. [[CrossRef](#)]
10. Díez-Pascual, A.M.; Díez-Vicente, A.L. Epoxidized Soybean Oil/ZnO Biocomposites for Soft Tissue Applications: Preparation and Characterization. *ACS Appl. Mater. Interfaces* **2014**, *6*, 17277–17288. [[CrossRef](#)] [[PubMed](#)]
11. Díez-Pascual, A.M.; Díez-Vicente, A.L. Wound Healing Bionanocomposites Based on Castor Oil Polymeric Films Reinforced with Chitosan-Modified ZnO Nanoparticles. *Biomacromolecules* **2015**, *16*, 2631–2644. [[CrossRef](#)] [[PubMed](#)]
12. Díez-Pascual, A.M. Antibacterial Activity of Nanomaterials. *Nanomaterials* **2018**, *8*, 359. [[CrossRef](#)]
13. Díez-Pascual, A.M.; Díez-Vicente, A.L. Antibacterial SnO₂ nanorods as efficient fillers of poly(propylene fumarate-co-ethylene glycol) biomaterials. *Mater. Sci. Eng. C* **2017**, *78*, 806–816. [[CrossRef](#)]
14. Díez-Pascual, A.M. State of the Art in the Antibacterial and Antiviral Applications of Carbon-Based Polymeric Nanocomposites. *Int. J. Mol. Sci.* **2021**, *22*, 10511. [[CrossRef](#)]
15. Finnveden, M.; Hendil-Forsell, P.; Claudino, M.; Johansson, M.; Martinelle, M. Lipase-Catalyzed Synthesis of Renewable Plant Oil-Based Polyamides. *Polymers* **2019**, *11*, 1730. [[CrossRef](#)] [[PubMed](#)]
16. Meier, M.A.R.; Metzger, J.; Schubert, U.S. Plant oil renewable resources as green alternatives in polymer science. *Chem. Soc. Rev.* **2007**, *36*, 1788–1802. [[CrossRef](#)] [[PubMed](#)]
17. Mosiewicki, M.A.; Aranguren, M.I. A short review on novel biocomposites based on plant oil precursors. *Eur. Polym. J.* **2013**, *49*, 1243–1256. [[CrossRef](#)]
18. Sharma, V.; Kundu, P.P. Condensation polymers from natural oils. *Prog. Polym. Sci.* **2008**, *33*, 1199–1215. [[CrossRef](#)]
19. Datta, J.; Glowinska, E. Chemical modifications of natural oils and examples of their usage for polyurethane synthesis. *J. Elastom. Plast.* **2014**, *46*, 33–42. [[CrossRef](#)]
20. Gurunathan, T.; Mohanty, S.; Nayak, S.K. Isocyanate terminated castor oil-based polyurethane prepolymer: Synthesis and characterization. *Prog. Org. Coat.* **2015**, *80*, 39–48. [[CrossRef](#)]
21. Petrovic, Z.S. Polyurethanes from vegetable oils. *Polym. Rev.* **2008**, *48*, 109–155. [[CrossRef](#)]
22. Danov, S.M.; Kazantsev, O.A.; Esipovich, A.L.; Belousov, A.S.; Rogozhina, A.E.; Kanakova, E.A. Recent advances in the field of selective epoxidation of vegetable oils and their derivatives: A review and perspective. *Catal. Sci. Technol.* **2017**, *7*, 3659–3675. [[CrossRef](#)]
23. Dinda, S.; Goud, V.V.; Patwardhan, A.V.; Pradhan, N.C. Selective epoxidation of natural triglycerides using acidic ion exchange resin as catalyst. *Asia-Pac. J. Chem. Eng.* **2011**, *6*, 870–878. [[CrossRef](#)]
24. Orellana Coca, C.; Billakanti, J.; Mattiasson, B.; HattiKaul, R. Lipase mediated simultaneous esterification and epoxidation of oleic acid for the production of alkylepoxystearates. *J. Mol. Catal. B Enzym.* **2007**, *44*, 133–137. [[CrossRef](#)]
25. Klaas, M.R.; Warwel, S. Complete and partial epoxidation of plant oils by lipase-catalyzed perhydrolysis. *Ind. Crop. Prod.* **1999**, *9*, 125–132. [[CrossRef](#)]
26. Husic, S.; Javni, I.; Petrovic, Z.S. Thermal and mechanical properties of glass reinforced soybased polyurethane composites. *Compos. Sci. Technol.* **2005**, *65*, 19. [[CrossRef](#)]
27. Das, R.; Kumar, R.; Banerjee, S.L.; Kundu, P.P. Engineered elastomeric bio-nanocomposites from linseed oil/organoclay tailored for vibration damping. *RSC Adv.* **2014**, *4*, 59265–59274. [[CrossRef](#)]
28. Pillai, A.M.; Sivasankarapillai, V.S.; Rahdar, A.; Joseph, J.; Sadeghfhar, F.; Rajesh, K.; Kyzas, G.Z. Green synthesis and characterization of zinc oxide nanoparticles with antibacterial and antifungal activity. *J. Mol. Struct.* **2020**, *1211*, 128107. [[CrossRef](#)]
29. Thielemans, W.; McAninch, I.M.; Barron, V.; Blau, W.J.; Wool, R.P. Impure carbon nanotubes as reinforcements for acrylated epoxidized soy oil composites. *J. Appl. Polym. Sci.* **2005**, *98*, 1325–1338. [[CrossRef](#)]
30. Zhang, C.Q.; Vennerberg, D.; Kessler, M.R. In situ synthesis of biopolyurethane nanocomposites reinforced with modified multiwalled carbon nanotubes. *J. Appl. Polym. Sci.* **2015**, *132*, 42515. [[CrossRef](#)]
31. Miyagawa, H.; Mohanty, A.K.; Drzal, L.T.; Misra, M. Nanocomposites from biobased epoxy and single-wall carbon nanotubes: Synthesis, and mechanical and thermophysical properties evaluation. *Nanotechnology* **2005**, *16*, 118–124. [[CrossRef](#)]
32. Wang, C.S.; Chen, X.Y.; Xie, H.F.; Cheng, R.S. Effects of carbon nanotube diameter and functionality on the properties of soy polyol-based polyurethane. *Compos. Part A* **2011**, *42*, 1620–1626. [[CrossRef](#)]
33. Rana, S.; Karak, N.; Cho, J.W.; Kim, Y.H. Enhanced dispersion of carbon nanotubes in hyperbranched polyurethane and properties of nanocomposites. *Nanotechnology* **2008**, *19*, 495707. [[CrossRef](#)]
34. Liang, K.; Shi, S.Q. Soy-based polyurethane foam reinforced with carbon nanotubes. *Key Eng. Mater.* **2010**, *419–420*, 477–480. [[CrossRef](#)]
35. Díez-Pascual, A.M.; Naffakh, M. Grafting of an aminated poly(phenylene sulphide) derivative to functionalized single-walled carbon nanotubes. *Carbon* **2012**, *50*, 857–868. [[CrossRef](#)]
36. Díez-Pascual, A.M. Chemical Functionalization of Carbon Nanotubes with Polymers: A Brief Overview. *Macromol* **2021**, *1*, 64–83. [[CrossRef](#)]
37. Kroto, H.W. C60: Buckminsterfullerene, The Celestial Sphere that Fell to Earth. *Ang. Chem. Int. Ed.* **1992**, *31*, 111–129. [[CrossRef](#)]

38. Díez-Pascual, A.M.; Díez-Vicente, A.L. Poly(propylene fumarate)/Polyethylene Glycol-Modified Graphene Oxide Nanocomposites for Tissue Engineering. *ACS Appl. Mater. Interfaces* **2016**, *8*, 17902–17914. [[CrossRef](#)]
39. Díez-Pascual, A.M.; Luceño Sánchez, J.A.; Peña Capilla, R.; García Díaz, P. Recent Developments in Graphene/Polymer Nanocomposites for Application in Polymer Solar Cells. *Polymers* **2018**, *10*, 217. [[CrossRef](#)]
40. Díez-Pascual, A.M.; González-Domínguez, J.M.; Martínez, M.T.; Gómez-Fatou, M.A. Poly(ether ether ketone)-based hierarchical composites for tribological applications. *Chem. Eng. J.* **2013**, *218*, 285–294. [[CrossRef](#)]
41. Díez-Pascual, A.M.; Gascón, D. Carbon Nanotube Buckypaper Reinforced Acrylonitrile–Butadiene–Styrene Composites for Electronic Applications. *ACS Appl. Mater. Interfaces* **2013**, *5*, 12107–12119. [[CrossRef](#)]
42. Díez-Pascual, A.M.; Shuttleworth, P.S.; González-Castillo, E.I.; Marco, C.; Gómez-Fatou, M.A.; Ellis, G. Polymer Blend Nanocomposites: Effect of Selective Nanotube Location on the Properties of a Semicrystalline Thermoplastic Toughened Epoxy Thermoset. *Macromol. Mater. Eng.* **2014**, *299*, 1430–1444. [[CrossRef](#)]
43. Díez-Pascual, A.M.; Naffakh, M. Towards the development of poly(phenylene sulphide) based nanocomposites with enhanced mechanical, electrical and tribological properties. *Mater. Chem. Phys.* **2012**, *135*, 348–357. [[CrossRef](#)]
44. In Het Panhuis, M.; Thielemans WI, M.; Minett, A.I.; Leahy, R.; Le Foulgoc, B.; Blau, W.J.; Wool, R.P. A Composite from Soy Oil and Carbon Nanotubes. *Int. J. Nanosci.* **2003**, *2*, 185–194. [[CrossRef](#)]
45. Tang, Q.; Li, Q.; Pan, C.; Xi, Z.; Zhao, L. Poly(acrylated epoxidized soybean oil)-modified carbon nanotubes and their application in epoxidized soybean oil-based thermoset composites. *Polym. Compos.* **2021**, *42*, 5774–5788. [[CrossRef](#)]
46. Khandelwal, V.; Sahoo, S.; Kumar, A.; Sethi, S.; Manik, G. Bio-sourced electrically conductive epoxidized linseed oil based composites filled with polyaniline and carbon nanotubes. *Compos. Part B* **2019**, *172*, 76–82. [[CrossRef](#)]
47. Ali, A.; Yusoh, K.; Hasany, S.F. Synthesis and physicochemical behaviour of polyurethane multiwalled carbon nanotubes nanocomposites based on renewable castor oil polyols. *J. Nanomater.* **2014**, *2014*, 564384. [[CrossRef](#)]
48. Wang, C.; Zhang, Y.; Lin, L.; Ding, L.; Li, J.; Lu, R.; He, M.; Xie, H.F.; Cheng, R.S. Thermal, mechanical, and morphological properties of functionalized graphene-reinforced bio-based polyurethane nanocomposites. *Eur. J. Lipid Sci. Tech.* **2015**, *117*, 1940–1946. [[CrossRef](#)]
49. Zhang, J.; Zhang, C.Q.; Madbouly, S.A. In situ polymerization of bio-based thermosetting polyurethane/graphene oxide nanocomposites. *J. Appl. Polym. Sci.* **2015**, *132*, 4175.
50. Wang, H.; Gupta, A.; Kim, B.S. Photo-crosslinked polymer networks based on graphene-functionalized soybean oil and their properties. *Korean J. Chem. Eng.* **2019**, *36*, 591–599. [[CrossRef](#)]
51. Thakur, S.; Karak, N. Bio-based tough hyperbranched polyurethane-graphene oxide nanocomposites as advanced shape memory materials. *RSC Adv.* **2013**, *3*, 9476–9482. [[CrossRef](#)]
52. Thakur, S.; Karak, N. Multi-stimuli responsive smart elastomeric hyperbranched polyurethane/reduced graphene oxide nanocomposites. *J. Mater. Chem. A* **2014**, *2*, 14867–14875. [[CrossRef](#)]
53. Ahn, B.K.; Sung, J.; Li, Y.H.; Kim, N.; Ikenberry, M.; Hohn, K.; Mohanty, N.; Nguyen, P.; Sreeprasad, T.S.; Kraft, S.; et al. Synthesis and characterization of amphiphilic reduced graphene oxide with epoxidized methyl oleate. *Adv. Mater.* **2012**, *24*, 2123–2129. [[CrossRef](#)]
54. Chieng, B.W.; Ibrahim, N.A.; Wan Yunus, W.M.Z.; Hussein, M.Z.; Silverajah, V.S.G. Graphene Nanoplatelets as Novel Reinforcement Filler in Poly(lactic acid)/Epoxidized Palm Oil Green Nanocomposites: Mechanical Properties. *Int. J. Mol. Sci.* **2012**, *13*, 10920–10934. [[CrossRef](#)] [[PubMed](#)]
55. Gogoi, P.; Boruah, M.; Bora, C.; Dolui, S.K. Jatropha curcas oil based alkyd/epoxy resin/expanded graphite (eg) reinforced bio-composite: Evaluation of the thermal, mechanical and flame retardancy properties. *Prog. Org. Coat.* **2014**, *77*, 87–93. [[CrossRef](#)]
56. Bystrzejewski, M.; Huczko, A.; Lange, H.; Drabik, J.; Pawelec, E. Influence of C60 and Fullerene Soot on the Oxidation Resistance of Vegetable Oils. *Fuller. Nanotub. Carbon Nonstruct.* **2007**, *15*, 427–438. [[CrossRef](#)]
57. Szczesniak, D.; Przybyłek, P. Oxidation Stability of Natural Ester Modified by Means of Fullerene Nanoparticles. *Energies* **2021**, *14*, 490. [[CrossRef](#)]
58. Manchado, M.L.; Valentini, L.; Biagiotti, J.; Kenny, J.M. Thermal and mechanical properties of single-walled carbon nanotubes–polypropylene composites prepared by melt processing. *Carbon* **2005**, *43*, 1499–1505. [[CrossRef](#)]
59. Blake, R.; Coleman, J.N.; Byrne, M.T.; McCarthy, J.E.; Perova, T.S.; Blau, W.J.; Fonseca, A.; Nagy, J.B.; Gun'ko, K. Reinforcement of poly(vinyl chloride) and polystyrene using chlorinated polypropylene grafted carbon nanotubes. *J. Mater. Chem.* **2006**, *16*, 4206–4213. [[CrossRef](#)]
60. Yang, B.-X.; Pramoda, K.P.; Xu, G.Q.; Goh, S.H. Mechanical Reinforcement of Polyethylene Using Polyethylene-Grafted Multi-walled Carbon Nanotubes. *Adv. Func. Mater.* **2007**, *17*, 2062–2069. [[CrossRef](#)]
61. Li, J. Simultaneous Improvement in the Tensile and Impact Strength of Polypropylene Reinforced by Graphene. *J. Nanomater.* **2020**, *2020*, 7840802.
62. Afzal, A.; Kausar, A.; Siddiq, M. Perspectives of polystyrene composite with fullerene, carbon black, graphene, and carbon nanotube: A review. *Polym.-Plast. Technol. Eng.* **2016**, *55*, 1988–2011. [[CrossRef](#)]
63. Suner, S.; Joffe, R.; Tipper, J.L. Ultra High Molecular Weight Polyethylene/Graphene Oxide Nanocomposites: Thermal, Mechanical and Wettability Characterisation. *Compos. Part B* **2015**, *78*, 185–191. [[CrossRef](#)]
64. Zhang, C.; Garrison, T.F.; Madbouly, S.A.; Kessler, M.R. Recent advances in vegetable oil-based polymers and their composites. *Prog. Polym. Sci.* **2017**, *71*, 91–143. [[CrossRef](#)]

-
65. Kiu, K.; Suzana, Y.; Chok, V.S.; Arpin, T.; Samion, S.; Kamil, R. Tribological Investigation of Graphene as Lubricant Additive in Vegetable Oil. *J. Phys. Sci.* **2017**, *28*, 257–267.
 66. Razak, I.H.A.; Ahmad, M.A.; Fuad, N.N.N.; Shahrudin, K.S. Tribological properties of palm oil bio-lubricant with modified carbon nanotubes. *Int. J. Eng. Technol.* **2018**, *7*, 133–137.
 67. Behl, M.; Lendlein, A. Shape-memory polymers. *Mater. Today* **2007**, *10*, 20–28. [[CrossRef](#)]
 68. Deka, H.; Karak, N.; Kalita, R.D.; Buragohain, A. Biocompatible hyperbranched polyurethane/multi-walled carbon nanotube composites as shape memory materials. *Carbon* **2010**, *48*, 2013–2022. [[CrossRef](#)]
 69. Skaltsas, T.; Stergiou, A.; Chronopoulos, D.D.; Zhao, S.; Sinohara, H.; Tagmatarchis, N. All-Carbon Nanosized Hybrid Materials: Fluorescent Carbon Dots Conjugated to Multiwalled Carbon Nanotubes. *J. Phys. Chem. C* **2016**, *120*, 8550–8558. [[CrossRef](#)]